SUPPLEMENTAL MATERIAL:
DIMENSIONS OF MARINE PHYTOPLANKTON DIVERSTY

Stephanie Dutkiewicz[1,2], Pedro Cermeno[3], Oliver Jahn[1], Mick Follows[1], Anna Hickman[4], Darcy Taniguchi[5], Ben Ward[4]

1. Department of Earth, Atmospheric and Planetary Sciences, Massachusetts Institute of Technology, Cambridge, MA, 02139, USA
2. Center for Climate Change Science, Massachusetts Institute of Technology, Cambridge, MA, 02139, USA
3. Institut de Ciencies del Mar, CSIC, 08003 Barcelona, Spain
4. Ocean and Earth Sciences, University of Southampton, National Oceanography Centre Southampton, Southampton, SO14 3ZH, United Kingdom.
5. Department of Biological Sciences, California State University San Marcos, San Marcos, CA, 92096, USA

Correspondence to: Stephanie Dutkiewicz (stephd@mit.edu)

Supplemental Text.

S1. Ecosystem model parametrization

S1.1. Phytoplankton Growth: Phytoplankton growth rates were parameterized as functions of maximum photosynthetic rate, local light, nutrients and temperature. As in Dutkiewicz et al (2015a), we follow Geider et al (1998) such that the growth rate for phytoplankton *j* is equal to the carbon-specific photosynthesis rate:

$$P_j^C = P_{mj}^C \left(1 - \exp \frac{-\varphi_{Ej}\theta_j}{P_{mj}^C}\right) \qquad \textit{Eq S1.1}$$

where $P_{mj}^C = P_{mmaxj}^C \gamma_j^R \gamma_j^T$ is light-saturated photosynthesis rate, $\varphi_{Ej}$is the scalar irradiance absorbed by each phytoplankton multiplied by the maximum quantum yield of carbon fixation, and θ_j is
Chl a : C for each phytoplankton, determined using Geider et al (1998). These functions are provided in Dutkiewicz et al (2015a).

Nutrient limitation of growth was determined by the most limiting resource,

$$\gamma_j^R = \min(R_1^{lim}, R_2^{lim}, \dots) \qquad \textit{Eq S1.2}$$

where the nutrients considered are phosphate, iron, silicic acid and dissolved inorganic nitrogen. The effect on growth rate of ambient phosphate, iron or silicic acid concentrations was represented by a Michaelis-Menten function:

$$R_i^{lim} = \frac{R_i}{R_i + k_{ij}} \qquad \textit{Eq S1.3}$$

where the k_{ij} were half-saturation constants for phytoplankton type *j* with respect to the ambient concentration of nutrient *i*. We resolved three potential sources of inorganic nitrogen (ammonia, nitrite and nitrate). Phytoplankton preferentially use ammonia (as described in Dutkiewicz et al. 2015a)

Each functional group had different values of maximum photosynthesis rate, P^C_{maxj} and, nutrient half-saturation, k_{ij} and potentially have different nutrient needs. For instance, diatoms were parameterized to required silicic acid, diazotrophs to fix nitrogen, and mixotrophic dinoflagellates to graze as well as photosynthesis.

Temperature modulation of growth was represented, as in Dutkiewicz et al (2015b), by a non-dimensional factor (Fig 3). This factor is a function of ambient temperature, *T (K)*:

$$\gamma_j^T = \tau_T \exp\left(A_T\left(\frac{1}{T} - \frac{1}{T_N}\right)\right)\exp(-B_T|T - T_{oj}|^b) \qquad \textbf{Eq S1.4}$$

Coefficient τ_T normalized the maximum value, while A_T, B_T, T_N, and *b* regulated the sensitivity envelope. T_{oj} sets the optimum temperature specific to each of the 10 thermal norms. There was an increase in maximum growth rate for types with higher optimum temperature as suggested by observations (Eppley, 1972; Bissenger et al., 2008), and a specific temperature range over which each type could grow also as suggested by observations (Boyd et al 2013; Thomas et al 2012). The norms are spread uniformly though the range of temperatures found in the model ocean.

S1.2. Size based parameters*:* Following Ward et al (2012), we scale several of the plankton growth and loss parameters (p) as a function of their volume: $p=aV^b$. These parameters are shown in Supplemental Table S1. Mostly these values for the phytoplankton are the same as in Ward et al (2012), and references for those values are given in that paper. However, we did not use the same values for maximum growth rates (μ_{max}). Here we particularly wish to capture the distinction between functional types (Fig 4a). We fit a and b to capture the top of the envelop of the observed maximum growth rates. For the pico-phytoplankton we use a positive slope as suggested by the observations from the smallest phytoplankton shown here and in several recent studies (Kempes et al, 2012; Bec et al 2008; Maranon et al, 2013). For the larger phytoplankton we use a negative b, but lower value than used in Ward et al (2012). The envelop is less steep, as in this model the effect of self-shading is also taking into effect (see below) and as such the realized growth is much lower for the largest size classes. This unimodal distribution of growth rates has been observed (e.g. Raven 1994; Bec et al 2008; Finkel et al 2010; Maranon et al 2013; Sal et al 2015) and explained as a tradeoff between replenishing cell quotas versus synthesizing new biomass (Verdy et al., 2009; Ward et al 2017).

Allometric relationships have been empirically determined for cell minimum stoichiometric quotas (Q_{min}), cell nutrient uptake half saturation constants (*K*), and cell nutrient uptake rates (V_{max}). Here we convert to the half saturation for growth (*k*) used in the model Monod formulation of growth rate following Follows et al (2018):

$$k = K\frac{\mu_{max}Q_{min}}{V_{max}} \qquad \textbf{Eq S1.5}$$

We calculate this for nitrate and use the cell elemental stoichiometry to calculate for each of the other nutrients.

S1.3. Phytoplankton absorption and scattering spectra: The model is forced by spectral irradiances in 25nm bands from 400 to 700nm from the Ocean-Atmosphere Spectral Irradiance Model (OASIM, Gregg 2001). As in Dutkiewicz et al (2015a) the phytoplankton absorb, scatter and backscatter the irradiance. The spectra for the functional groups are similar to those used in Dutkiewicz et al (2015a), but here we introduce parameterization to capture the changes in the spectra for different size classes (Supplemental Fig S1). For simplicity the different pico-phytoplankton and diazotrophs are not assumed to have differences in accessory pigments as was done in Dutkiewicz et al (2015a).

A representative light absorption spectrum for each functional group was selected from representative species in culture (as in Dutkiewicz et al. 2015a). The spectra were then scaled by cell size by applying the allometric relationship of Finkel et al. (2000) at each wavelength. A representative scattering spectrum and ratio of backward to forward scattering for each functional group was also selected from representative species in culture (as in Dutkiewicz et al. 2015a). The representative spectra were scaled through the range of cell sizes using the allometric scaling exponent found for the dataset of Stramski et al. 2001 (and assuming cell carbon to volume ratio of Montagnes et al. 1994). The size scaling exponent was found for each wavelength. A different exponent for the smaller (less than ~2 um) and larger cells was also applied given the different exponents evident in the dataset. The backscatter to total scattering ratios for representative spectra were assumed spectrally independent (Dutkiewicz et al. 2015a) and scaled through the range of cell sizes by the allometric exponent found for the dataset in Stramski et al. (2001): $\log(bb/\bar{b})/\log(d_j)$ = -1.46, where *bb* is backscatter spectrum, $\bar{b}$ is mean backscatter an d_j is diameter of cell *j*).

S1.4. Grazing: Grazing is represented as a Holling III function (Holling, 1959), such that the grazer *k* preys on plankton *j* as

$$g_{jk} = g_{maxk}\gamma_{zk}^{T}\frac{\sigma_{jk}B_j}{G_k}\frac{G_k^2}{G_k^2+k_p^2} \qquad \textbf{Eq S1.6}$$

where g_{maxk} is the maximum grazing rate of grazer *k*, B_j is biomass of prey *j*, k_p is the grazing half saturation rate, and σ_{jk} is the palability of phytoplankton *j* to grazer *k*. G_j is the palability weighted total phytoplankton biomass: $\sum_j \sigma_{jk}B_j$. Temperature modulation of grazing, γ_{zk}^{T}, has a similar exponential increase with temperature, T, as for phytoplankton growth (Eq S1.4), but without specific ranges: $\gamma_{zk}^{T} = \tau_T \exp\left(A_T\left(\frac{1}{T}-\frac{1}{T_N}\right)\right)$ where coefficient τ_T normalized the maximum value, while A_T sets the sensitivity.

The matrix of palatability is set such that grazers prefer prey 10 times smaller than themselves (Fenchel 1987; Kiorboe 2008, Ward et al., 2012, Baird et al., 2004), but they also graze on one size class lower and higher (i.e from 5-20 times smaller than themselves). Diatoms and coccolithophores, with their hard shells

that are likely defensive (Monteiro et al 2017, Pančić et al 2019) are assumed 10% less palatable than other phytoplankton.

Maximum grazing rates were guided by compilation of observations from Taniguchi et al. (2014) and Jeong et al. (2010) (Supplemental Fig S2). All grazing rate values were temperature corrected to 20°C using a Q_{10} value of 2.8 (Hansen et al., 1997). We chose a size-independent maximum grazing rate for the four smallest zooplankton (following from lack of size dependence observed for nanoflagellates' maximum grazing rates), and slower grazing with size for the larger zooplankton (Supplemental Table S1). Data from Jeong et al. (2010) was used to differentiation between mixotrophic and heterotrophic dinoflagellates. Here we assume that mixotrophs have a lower maximum grazing rate than other grazers of the same size (Jeong et al 2010; Supplemental Fig S2). Observations of k_p do not suggest a strong size dependence, and as such we use the same value for all grazers.

S2. Shannon Index

Though richness is a more applicable measure of diversity for this study, where our theory determines co-existence, here we also provide the Shannon Index (*H*). Shannon diversity is determined as:

$$H = -\sum_j \frac{B_j}{B_{TOT}} \ln \frac{B_j}{B_{TOT}} \qquad \textit{Eq. S2.1}$$

Where B_j is the biomass of the *j*-th phytoplankton class, group, or norm (depending on whether considering total, size, functional, or thermal Shannon index), and biomass of all the phytoplankton is B_{TOT}. Shannon diversity therefore also includes a measure of how evenly the biomass is distributed. A higher Shannon index suggests a more evenly distributed community. We show these here normalized to the maximum value for each dimension (or total), that is if the biomass was evenly distributed between all types/classes/groups/norms (depending on which dimension). We find that size classes have the highest Shannon over most of the globe, while the temperature norms have the lowest Shannon (Supplemental Fig S8).

Supplemental References

Baird, M.E., One, R.R., Suthers, I.M., & Middleton, J.H. 2004. A plankton population model with biomechanics descriptions of biological processes in an idealized 2D ocean basin. *J. Mar, Sys.* **50**, 199-222 (2004)

Bec, B., Collos, Y., Vaquer, A. et al. Growth rate peaks at intermediate cell size in marine photosynthetic picoeukaryotes. *Limnol. Oceanogr*., **53**, 863–867 (2008)

Bissenger, J.E., Montagnes, D.J.S., Harples, J., & Atkinson, D. Predicting marine phytoplankton maximum growth rates from temperature: Improving on the Eppley curve using quantile regression, *Limnol. Oceangr.***, 53**, 487-493 (2008)

Boyd et al. Marine phytoplankton temperature verus growth response from polar to tropical waters – outcome of a scientific community-wide study. *PlosOne*, **8**(5), e63091 (2013)

Dutkiewicz, S., Hickman, A.E., Jahn, O., Gregg, W.W., Mouw, C.B. & Follows, M.J. Capturing optically important constituents and properties in a marine biogeochemical and ecosystem model. *Biogeoscience*, **12**, 4447-4481 doi:10.5194/bg-12-4447-2015 (2015a)

Dutkiewicz, S., Morris, J., Follows, M.J., Scott, J., Levitan, O., Dyhrman, S. & Berman-Frank, I. Impact of ocean acidification on the structure of future phytoplankton communities *Nature Climate Change***,** doi:10.1038/nclimate2722 (2015b)

Eppley, R. W. Temperature and phytoplankton growth in the sea, *Fish. B.,* **70**, 1063–1085 (1972)

Fenchel, T. *Ecology—Potentials and Limitations.* Excellence in Ecology: Book 1. Otto Kinne (ed). Ecology Institute. 187 pp. (1987)

Finkel, Z. and AJ Irwin (2000) Modeling size-dependent photosynthesis: light absorption and the allometric rule. *J. theor. Biol.* **204**: 361-369. 10.1006/jtbi.2000.2020

Finkel, Z. V., J. Beardall, J., Flynn, K.J., Quigg, A., Rees, T.A.V., & Raven, J.A.. Phytoplankton in a changing world: cell size and elemental stoichiometry. *J. Plankton Res.* **32**, 119–137 (2010)

Geider, R. J., MacIntyre, H. L., & Kana, T. M. A dynamic regulatory model of photoacclimation to light, nutrient and temperature, *Limnol. Oceanogr.*, **43**, 679–694 (1998)

Gregg, W. W.A Coupled Ocean–Atmosphere Radiative Model for Global Ocean Biogeochemical Model, NASA Technical Report Series on Global Modeling and Data Assimilation, NASA/TM-2002-104606, **22**, NASA, Goddard Space Flight Center, Greenbelt, MD (2002)

Holling, C. S. Some characteristics of simple types of predation and parasitism, *Canadian Entomologist*, ***91***(7), 385-398 (1959)

Jeong, H.J., Yoo Y.D., Kim, J.S., Seon K.A., Kang, N.S., & Kim, T.H. Growth, Feeding and Ecological Roles of the Mixotrophic and Heterotrophic Dinoflagellates in Marine Planktonic Food Webs. *Ocean Sci. J.* **45**(2):65-91, doi: 10.1007/s12601-010-0007-2 (2010)

Kempes, C.P., Dutkiewicz, S. &Follows, M.J. Growth, metabolic partitioning, and the size of microorganisms. *Proceedings of the National Academy of Science*, **109**, 495-500, doi:10.1073/pnas.1115585109 (2012)

Kiorboe, T. *A mechanistic approach to plankton ecology.* Princeton University Press. 224 pp (2008)

Hansen, B.B., Bjornsen, B.W., & Hansen, P.J. Zooplankton grazing and growth: Scaling within the 2– 2000 mm body size range. *Limnol. Oceanogr*. **42**, 687–704, doi:10.4319/lo.1997.42.4.0687 (1997)

Maranon E, Cermeno P, Lopez-Sandoval DC, Rodrıguez-Ramos T, Sobrino C, et al. Unimodal size scaling of phytoplankton growth and the size dependence of nutrient uptake and use. *Ecol Lett* **16**: 371–379 (2013)

Monteiro, F.M., Bach, L.T., Brownlee, C., Brown, P., Rickaby, R.E.M., Tyrrell, T., Beaufort, L., Dutkiewicz, S., Gibbs, S., Gutowska, M.A., Lee, R., Poulton, A.J., Riebesell, U., Young, J., Ridgwell, A. Why marine phytoplankton calcify? S*cience Advances*, **2**, doi: 0.1126/sciadv.1501822 (2016).

Pančić, M., Rodriguez Torres, R., Almeda, R., & Kiørboe, T. Silicified cell walls as a defensive trait in diatoms**.** *Proceedings of the Royal Society B: Biological Sciences, **286**,* doi.org/10.1098/rspb.2019.0184 (2019)

Raven, J. A.: Why are there no picoplanktonic O2 evolvers with volumes less than 10^{-19} m^3? *Journal of Plankton Research*, **16**, 565– 580, 1994.

Sal, S., L. Alonso-Sáez, L., Bueno, J., García, F.C. & López-Urrutia, A. Thermal adaptation, phylogeny, and the unimodal size scaling of marine phytoplankton growth. *Limnol. Oceanogr.*, **60**, 1212–1221 (2015)

Stramski, D., Bricaud, A., & Morel, A. Modeling the inherent optical properties of the ocean based on the detailed composition of the planktonic community, *Appl. Optics*, **40,** 2929–2945 (2001).

Taniguchi, D.A.A.**,** M.R. Landry, P.J.S. Franks, & K.E. Selph. Size-specific growth and grazing rates for picophytoplankton in coastal and oceanic regions of the eastern Pacific. *Marine Ecology Progress Series*. **509**, 87-101 (2014)

Thomas, M.K., Kremer C.T., Klausmeier C.A., & Litchman E. A global pattern of thermal adaptation in marine phytoplankton. *Science*, **336**, 1085-1088, doi.10.1126/science.1224836 (2012)

Verdy, A., Follows, M.J., & Flierl, G. Evolution of phytoplankton cell size in an allometric model. *Marine Ecology Progress Series*, **379**, 1-12 (2009)

Ward, B.A., Dutkiewicz, S., Jahn, O. & Follows, M.J. A size-structured food-web model for the global ocean. *Limnol. Oceanogr.*, **57**, 1877-1891 (2012)

Ward B.A., Marañón E., Sauterey B., Rault J. & Claessen C. The size-dependence of phytoplankton growth rates: a trade-off between nutrient uptake and metabolism. The American Naturalist, **189** (2), 170-177 (2017)

Supplemental Table

		a	b	Units
maximum growth rate, μ_{max}	Pico cocco diazotroph diatom dinoflagellates	0.9 1.4 0.95 3.9 1.7	0.8 -0.8 -0.8 -0.8 -0.8	1/d
nutrient uptake half saturation constant, K	NO_3	0.17	0.27	mmol N/m^3
minimum cell quota relative to C, Q_{min}	N	0.07	-0.17	mmol N/mmol C
maximum nutrient uptake rate, V_{max}	NO3	0.51	-0.27	mmol N/mmol C/d
sinking	phytoplankton zooplankton	0.28 0.00	0.39	m/d
maximum grazing rate, g_{max}	dinoflagellates zooplankton<30um zooplankton>30um	10.3 9.8 30.9	-0.16 0.00 -0.16	1/d

Supplemental Table S1: Plankton parameters that scale with size. Parameter=aV^b

Supplemental Figures.

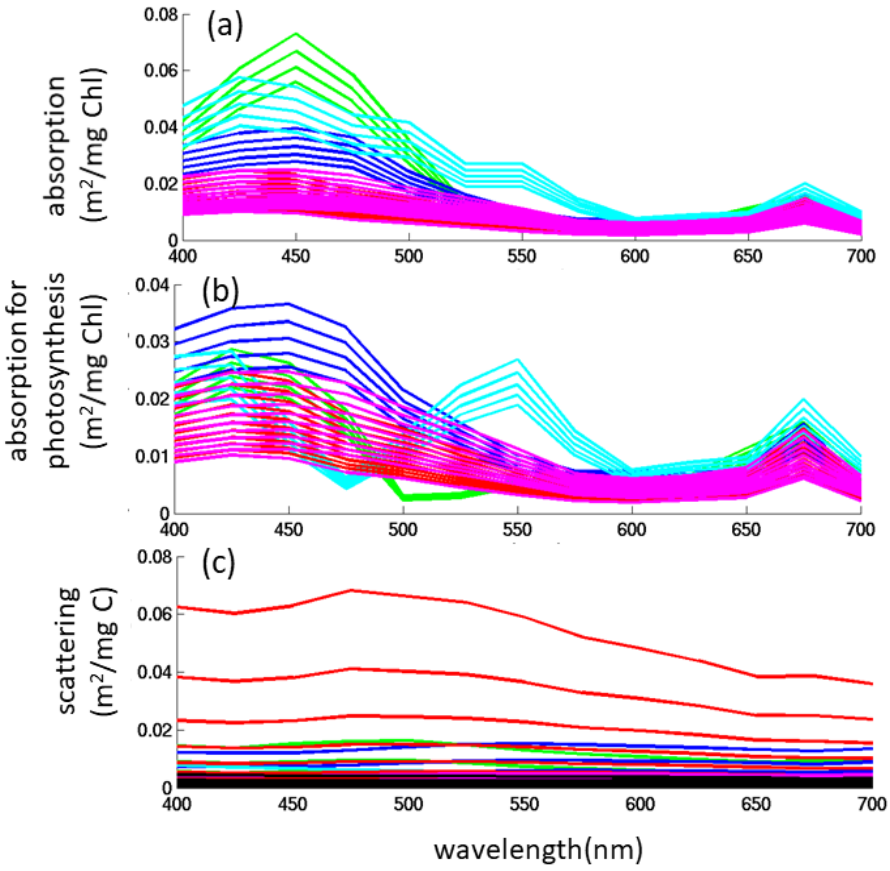

Supplemental Figure S1: Absorption and scattering spectra. (a) Chl a-specific total absorption by phytoplankton (m^2/mg Chl a); **(b)** Chl a-specific absorption by photosynthetic pigments (m^2/mg Chl); and **(c)** biomass specific scattering by phytoplankton (m^2/mgC). Same coloured lines show each size classes within functional group: red=diatoms; purple=mixotrophic dinoflagellates; dark blue=coccolithophores; light blue=diazotrophs; green=pico-phytoplankton; black=zooplankton (only scattering).

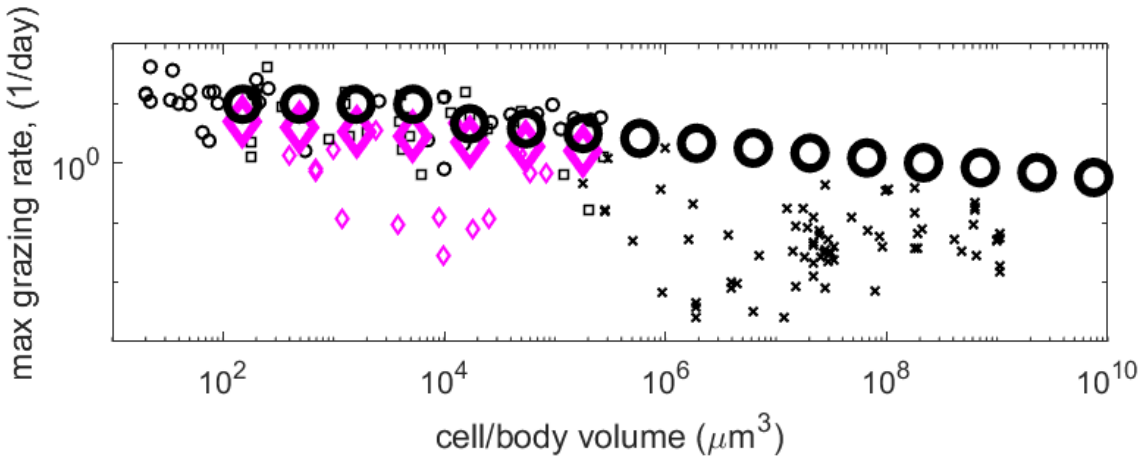

Supplemental Figure S2: Maximum grazing rate as a function of size. Small symbols indicate results from laboratory experiments, compiled by Taniguchi et al. (2014), Jeong et al., (2010) and Hansen et al (1997). Values were Q_{10} temperature corrected to 20°C using value of 2.8 (Hansen et al., 1997). Purple diamonds indicate mixotrophic dinoflagellates, black square for heterotrophic dinoflagellates, black circles for other protisan grazers, black crosses for metazoan grazers. Note that these metazoans from Hansen et al (1997) are mostly coastal species and many have non-planktonic life stages; the open ocean groups that the model is attempting to capture are therefore not represented here. The large black circles indicate the parameter values for the 16 model zooplankton size classes (the model does not differentiate between functional groups of heterotrophic zooplankton). The large purple diamonds indicate the values used for the model mixotrophic dinoflagellates.

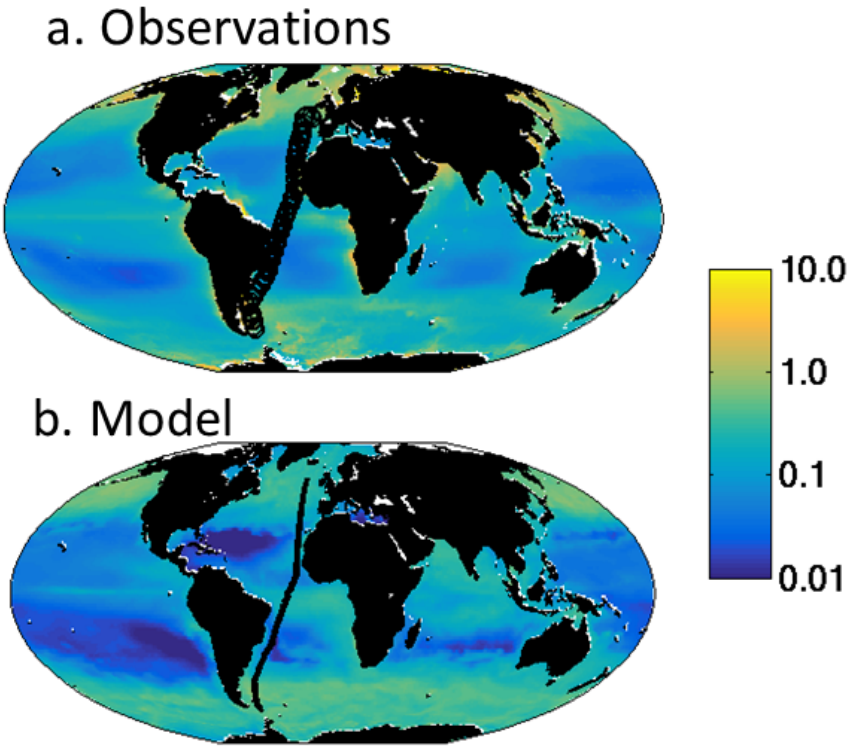

Supplemental Figure S3: Surface Chl-a (mg /m^3). (a) Observations satellite derived Chl-a and (b) from Model. The observations in (a) are an annual climatology of all satellite measurements, but miss observations in the polar winters; while (b) is an annual mean. Transect of the Atlantic Meridional Transect (AMT) are shown. Satellite observations are from Ocean Ocean Colour Climate Change Initiative project (OC-CCI, https://www.oceancolour.org/)

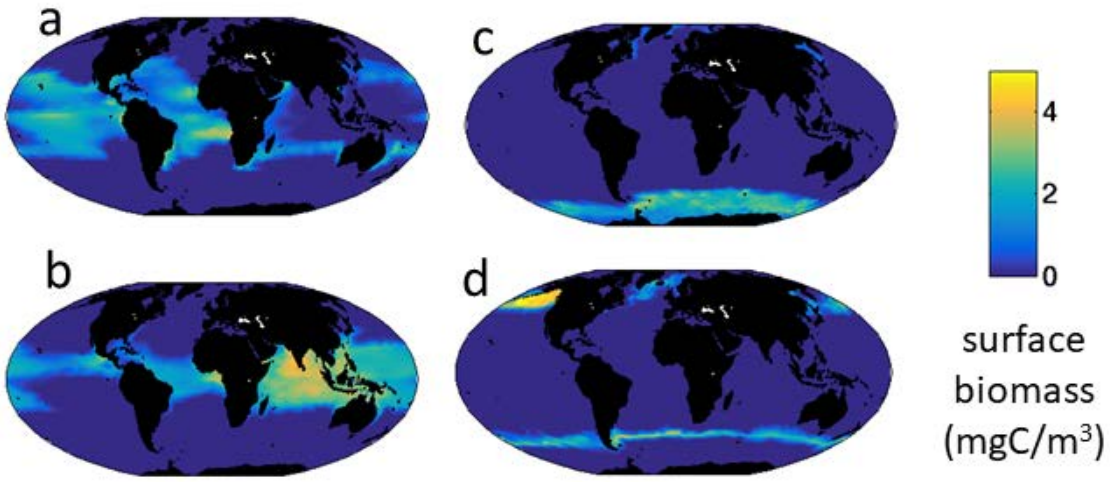

Supplemental Figure S4: Representative phytoplankton type distributions. Surface annual mean biomass (mgC/m3) of four of of the 350 types distributions. (a) and (b) are warm adapted small prokaryotes, (c) and (d) are cold adapted small diatoms. These are the types indicated with A,B,C,D in Fig 6.

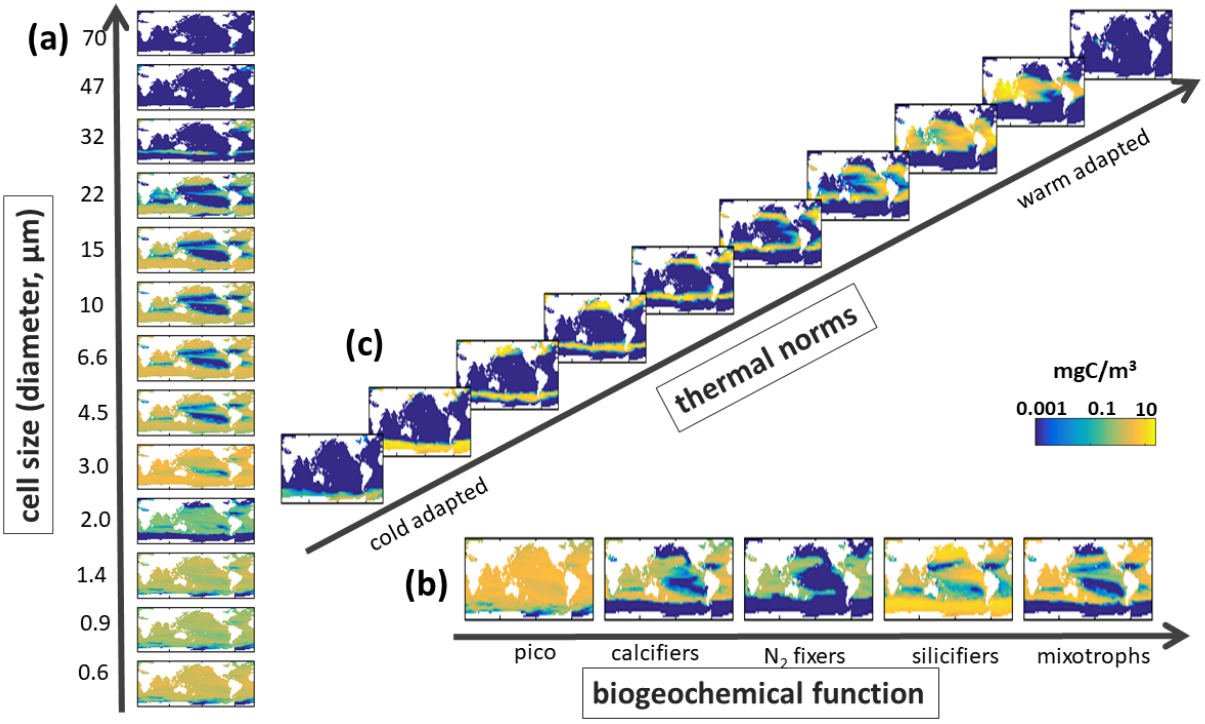

Supplemental Figure S5. Distributions along trait axes: Annual mean carbon biomass (mg C/m^3) over top 100m of (a) Sizes classes with equivalent spherical diameters (ESD) as labelled on Y-axis, shown is the sum across all functional groups and all temperature norms in that size classes; (b) Biogeochemical functional groups (pico-phytoplankton, coccolithophores, diazotrophs, diatoms and mixotrophic dinoflagellates) summed across all size classes and all temperature norms in those groups; and (c) thermal norms from coldest adapted to warm adapted (see Fig 3), summed across all functional groups and size class.

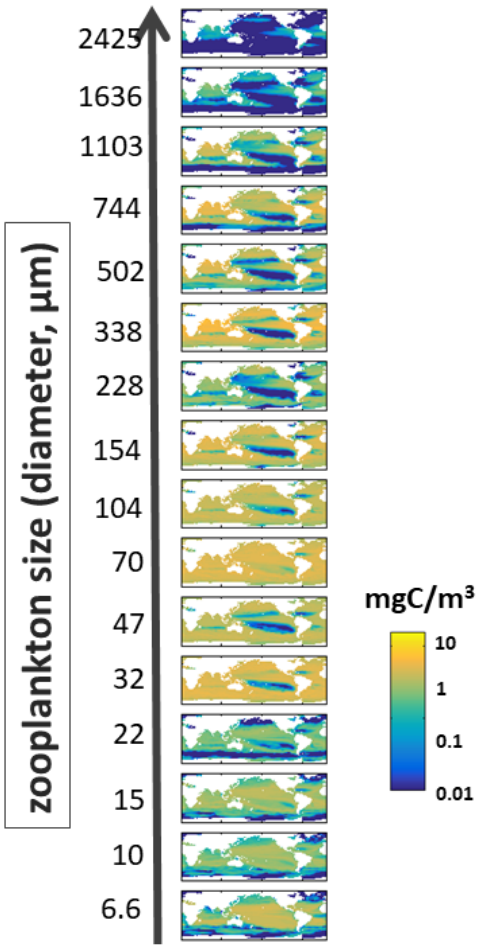

Supplemental Figure S6. Default model zooplankton biomass (mgC/m^3). Arranged by size (given as equivalent spherical diameter, ESD, on Y axis).

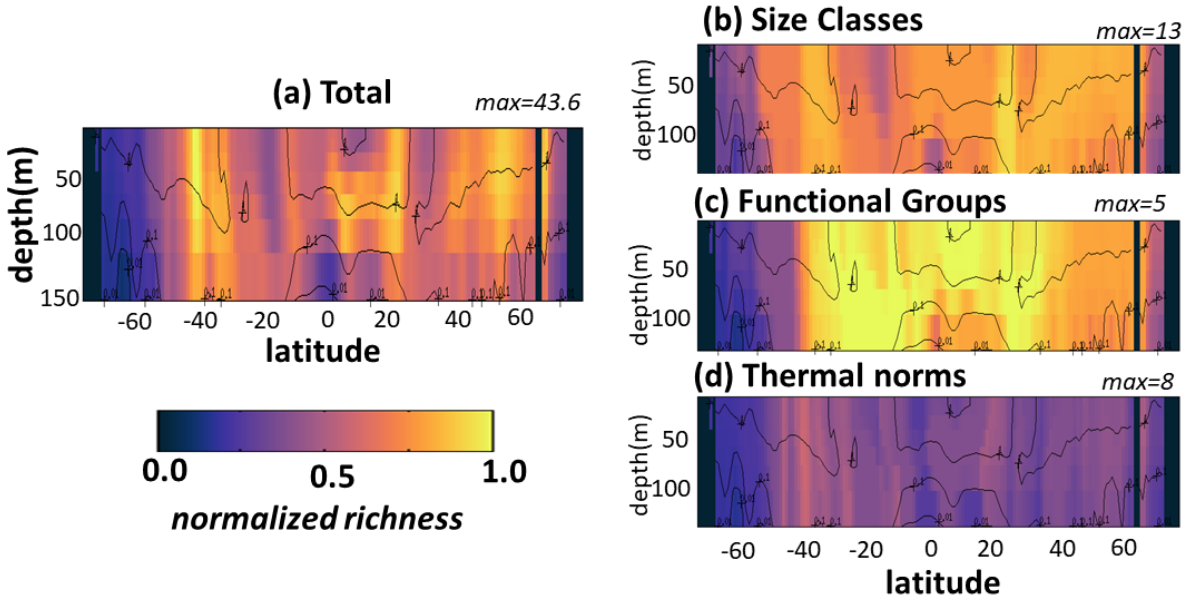

Supplemental Figure S7. Default model diversity measured as annual mean normalized richness with depth along a transect at 30W in the Atlantic Ocean. Normalization is the maximum in the transect for the total or the particular dimension. (a) total richness determined by number of individual phytoplankton types (of the 350) that co-exist at any location; (b) size class richness determined by number of co-existing size classes; (c) functional richness determined by number of co-existing biogeochemical functional groups; (d) thermal richness determined by number of co-existing temperature norms. Total richness (a) is a multiplicative function of the three sub-richness categories (b-d). Contours indicate total phytoplankton carbon biomass. Black indicates land/islands.

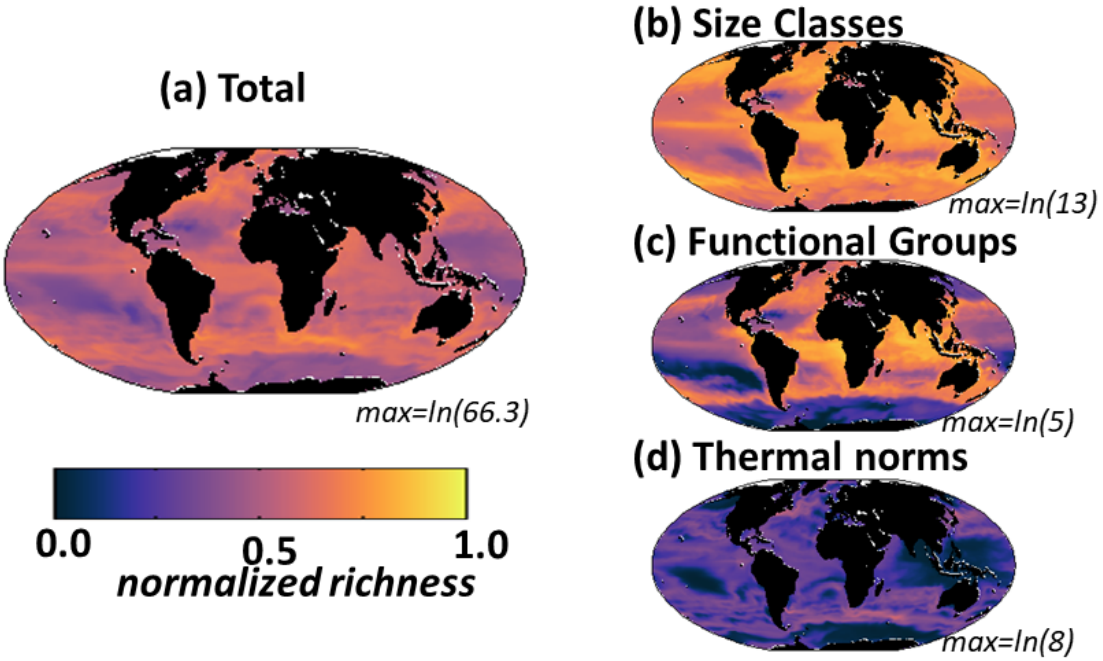

Supplemental Figure S8. Default model normalized annual mean Shannon diversity at the surface. (a) total Shannon; (b) size class shannon determined from co-existing size classes; (c) functional Shannon determined from co-existing biogeochemical functional groups; (d) thermal Shannon determined from co-existing temperature norms. All panels are normalized to the maximum value for that dimension (or total) as natural log of the maximum number of potentially coexisting types/classes/groups/norms.

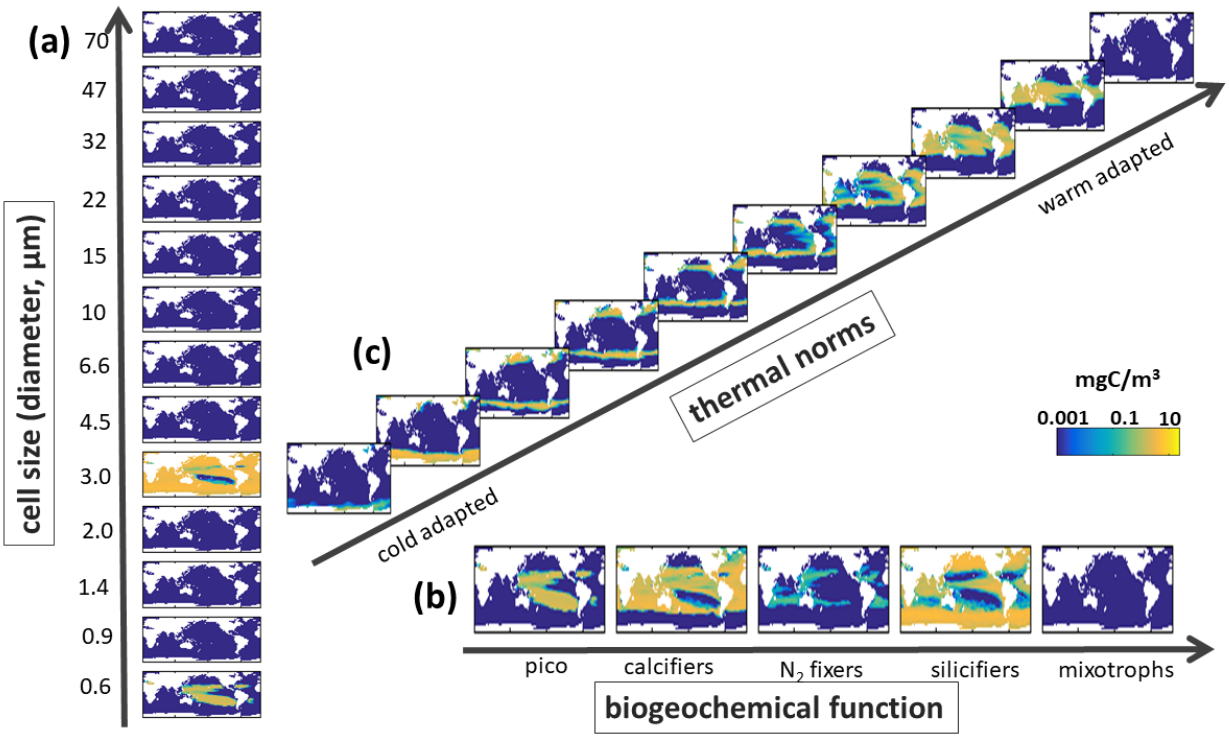

Supplemental Figure S9. EXP-1 Model Dimensions of Diversity: Sensitivity experiment where there is no mixotrophy and only a single grazer type preys on all phytoplankton. Annual mean carbon biomass (mg C/m^3) over top 100m of (a) Sizes classes with equivalent spherical diameters (ESD) as labelled on Y-axis, shown is the sum across all functional groups and all temperature norms in that size classes; (b) Biogeochemical functional groups (pico-phytoplankton, coccolithophores, diazotrophs, diatoms and dinoflagellates) summed across all size classes and all temperature norms in those groups; and (c) thermal norms from coldest adapted to warm adapted (see Fig 3), summed across all functional groups and size classes. Compare to Supplemental Fig S5.

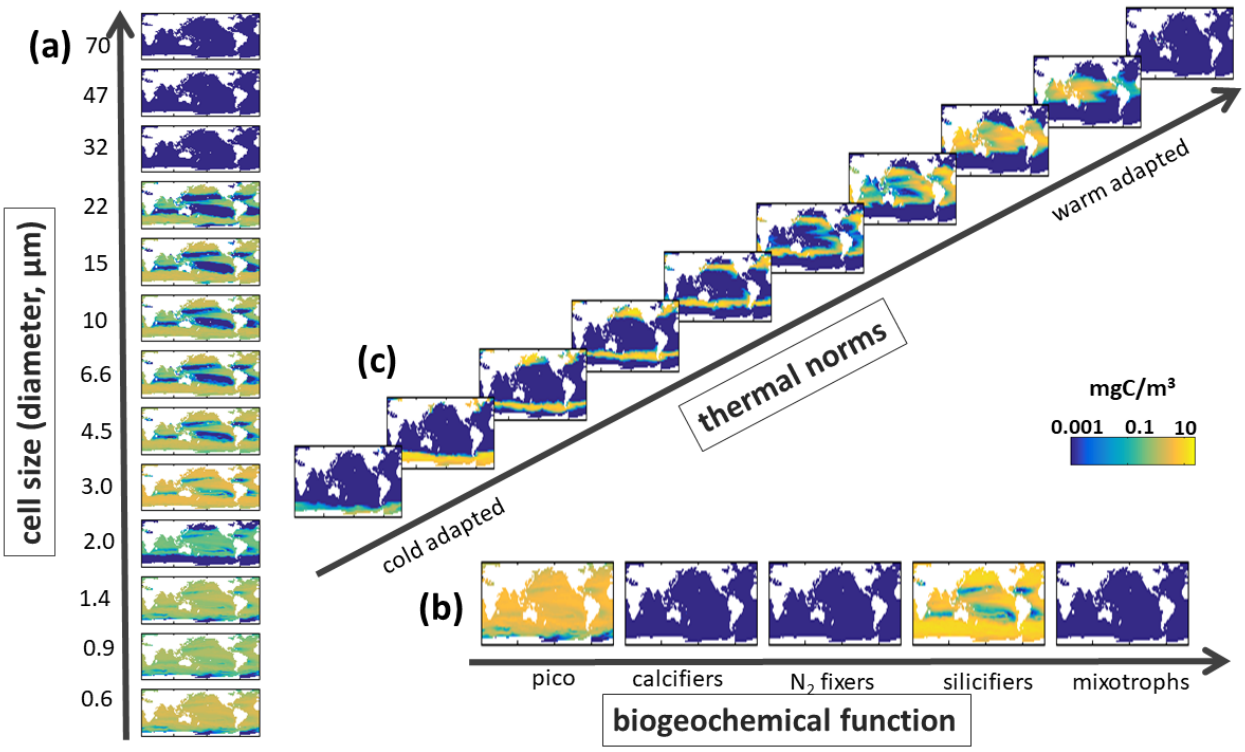

Supplemental Figure S10. EXP-2 Model Dimensions of Diversity. Sensitivity experiment where nutrient requirements are the same between functional group. Annual mean carbon biomass (mg C/m^3) over top 100m of (a) Sizes classes with equivalent spherical diameters (ESD) as labelled on Y-axis, shown is the sum across all functional groups and all temperature norms in that size classes; (b) Biogeochemical functional groups (pico-phytoplankton, coccolithophores, diazotrophs, diatoms and dinoflagellates) summed across all size classes and all temperature norms in those groups; and (c) thermal norms from coldest adapted to warm adapted (see Fig 3), summed across all functional groups and size classes.

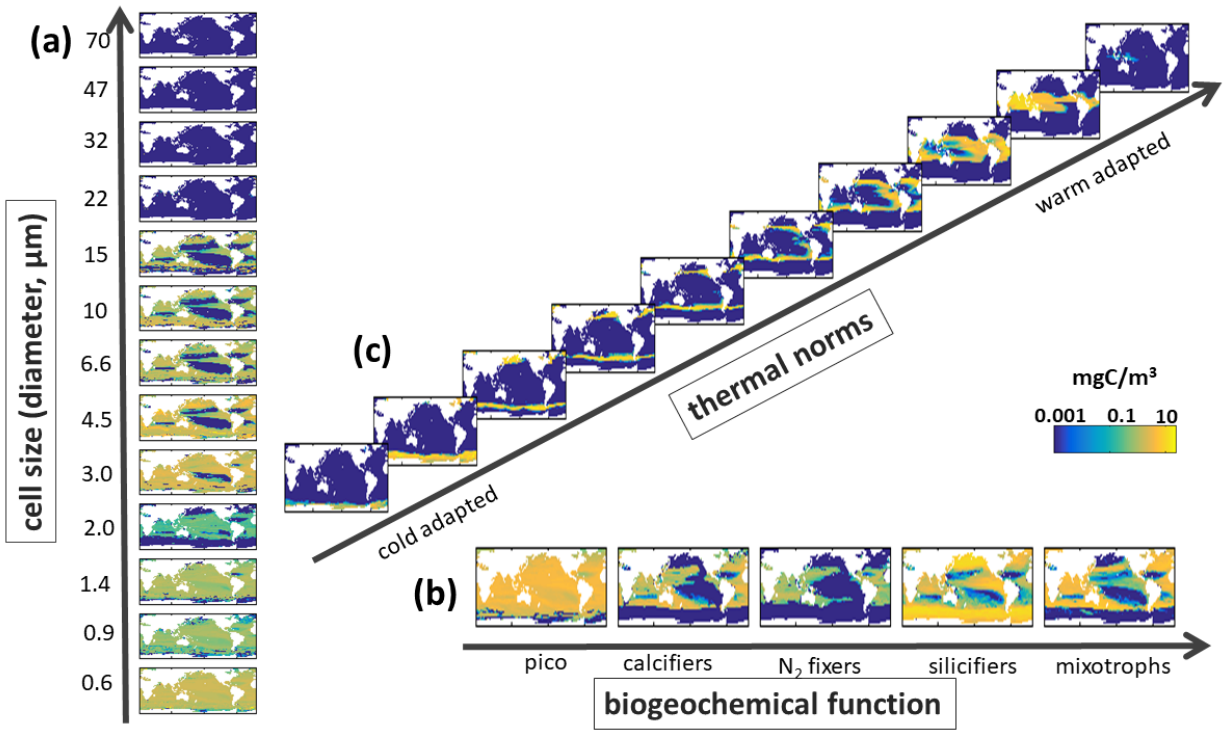

Supplemental Figure S11. EXP-3 Model Dimensions of Diversity: Sensitivity experiment where there is no horizontal transport of plankton; nutrients and dissolved and detrital organic matter are transported as in the default experiment. Annual mean carbon biomass (mg C/m^3) over top 100m of (a) Sizes classes with equivalent spherical diameters (ESD) as labelled on Y-axis, shown is the sum across all functional groups and all temperature norms in that size classes; (b) Biogeochemical functional groups (pico-phytoplankton, coccolithophores, diazotrophs, diatoms and dinoflagellates) summed across all size classes and all temperature norms in those groups; and (c) thermal norms from coldest adapted to warm adapted (see Fig 3), summed across all functional groups and size classes.